

MEASUREMENT OF MAGNETIC FIELD STRENGTH IN THE DARK CLOUD BARNARD 1

A. A. GOODMAN,^{1,2} R. M. CRUTCHER,³ C. HEILES,⁴ P. C. MYERS,² AND T. H. TROLAND⁵

Received 1988 August 30; accepted 1988 December 13

ABSTRACT

We report the detection of a $-27 \pm 4 \mu\text{G}$ magnetic field in the molecular cloud Barnard 1 (B1), via observations of the Zeeman effect in the 1665 and 1667 MHz lines of OH at the Arecibo 305 m telescope. The region of OH emission in B1 extends over 1.1 pc, has 1.3 km s^{-1} line width, and has mean column density $6 \times 10^{21} \text{ cm}^{-2}$. Detection of the Zeeman effect in this region represents one of the first field strength measurements directly relevant to a dense part of a region of low-mass star formation. Substitution of the OH line width, size, and column density information into models based on comparable magnetic, kinetic, and gravitational energy density in the cloud gives two independent field strength estimates, each $\sim 25 \mu\text{G}$, in agreement with the measured value. Substitution of other molecular line data, which pertain to larger ($\sim 3 \text{ pc}$; ^{13}CO) and smaller ($\sim 0.2 \text{ pc}$; NH_3) size scales, into the same equilibrium models give field strengths from 21 to $37 \mu\text{G}$, a range which may be insignificant compared to measurement error. The observed field strength is also consistent with a constant-mass equilibrium model of cloud evolution. B1 has an embedded low-luminosity ($3 L_{\odot}$) IRAS source and is one of many similar condensations in Perseus. The Perseus complex may thus prove useful for studies of the role of magnetic fields in the formation of low-mass stars.

Subject headings: interstellar: matter — magnetic fields

I. INTRODUCTION

Evidence is increasing for the idea that magnetic fields play a key role in the support and dynamics of molecular clouds. At optical, infrared, and submillimeter wavelengths, polarization measurements indicate the presence of magnetically aligned dust grains (Vrba, Strom, and Strom 1976; Tamura *et al.* 1987; Hildebrand 1988). Models that equate cloud magnetic, gravitational, and/or kinetic energy successfully predict observed relations among velocity dispersion, cloud size, and density (Myers and Goodman 1988*a, b*, hereafter MGa and MGb and references therein). And, in the increasing number of clouds with magnetic field strength measurements (Heiles 1987; Crutcher 1988), the same models correctly predict the measured field strength (MGa).

Nearby dark clouds are useful for analyzing optical polarization, cloud kinetic and gravitational energy, and conditions associated with low-mass star formation. Yet few magnetic field strength measurements are available in the dense parts of dark clouds. There, densities $n \gtrsim 10^3 \text{ cm}^{-3}$ are best traced by the 18 cm OH lines in emission, rather than in absorption (Graedel, Langer, and Frerking 1982). Only one detection of the Zeeman effect in OH emission from a dark cloud is known: Crutcher *et al.* (1989) measured $10 \pm 3 \mu\text{G}$ in the Ophiuchus dark cloud. Many similar detection efforts have failed, possibly because the OH emission has been beam-diluted, or integration times were insufficient to detect weak fields. In this *Letter* we report detection of the Zeeman effect in OH emission in the dark cloud Barnard 1 (B1). We minimized beam dilution with the high angular resolution of the 305 m Arecibo telescope.⁶

Lang and Willson (1979) attempted to detect the Zeeman effect at Arecibo in OH emission from gas associated with T Tauri stars. Their observations yielded no detections, but did give some important upper limits, including a 3σ limit of $90 \mu\text{G}$ at the position of LkH α 327, only $4'$ from position we observed in B1. The field strength we detected in B1, $-27 \pm 4 \mu\text{G}$, agrees well with two estimates of equilibrium field strength derived from our observations, and also with the evolutionary model of Mouschovias (1976*a, b*; 1987*a, b*).

II. OBSERVATIONS

The 1665 and 1667 MHz transitions of OH were observed at the 305 m Arecibo telescope during January and February of 1988. At the OH frequencies, using a 12 m line feed, the FWHM beamwidth of the telescope is $2.9'$. The time average of the system temperature was approximately 50 K.

For our Zeeman experiment, where isolating polarizations is crucial, polarization "switching" was employed at 1 Hz between right and left circular polarizations. A double-pole double-throw switch, with remotely adjustable gain in each signal path, was constructed by the NAIC staff for our experiment and installed between the last RF amplifier and the mixer. Use of this switch allowed the high time efficiency of dual-polarization observation, and also the cancellation of any differences in spectral response between the two signal paths following the switch. We also switched the local oscillator frequency by half the bandwidth every 3 minutes during Zeeman observations, and more often during mapping observations. The 1024 channel digital autocorrelator was split into four segments, each with 312.5 kHz bandwidth, to allow simultaneous observation of the 1665 and 1667 MHz lines in each polarization, with channel separation 0.22 km s^{-1} .

The molecular cloud core around the H II region S88B (cf. Crutcher, Kazès, and Troland 1987) was observed to test the measurement setup. We detected a magnetic field of $47 \pm 4 \mu\text{G}$ in 40 minutes of integration.

We surveyed about 40 molecular clouds in Perseus, Taurus, and Monoceros for OH emission, to an rms noise level of ~ 0.1

¹ Department of Physics, Harvard University.

² Harvard-Smithsonian Center for Astrophysics.

³ Department of Astronomy, University of Illinois.

⁴ Astronomy Department, University of California, Berkeley.

⁵ Department of Physics and Astronomy, University of Kentucky.

⁶ The Arecibo Observatory is part of the National Astronomy and Ionosphere Center (NAIC), which is operated by Cornell University under contract with the National Science Foundation.

TABLE 1
LINE-OF-SIGHT COMPONENT OF MAGNETIC FIELD STRENGTH DERIVED FROM ZEEMAN SPLIT OF
THE 18 CENTIMETER LINES OF OH

SOURCE	R.A.(1950)	DECL.(1950)	$B_{\parallel}(\mu\text{G})$		
			1665 MHz	1667 MHz	Combined
B1	3 ^h 30 ^m 12 ^s .0	30°57'26"	-27 ± 5	-25 ± 5	-27 ± 4
Taurus 16	4 15 01.0	28 16 00	<24	<27	<18
NGC 2264	6 38 10.0	9 37 30	<24	<21	<15
S88B	19 44 42.0	25 05 30	46 ± 3	48 ± 4	47 ± 3

NOTE.—The sign of B_{\parallel} indicates its direction: negative means toward the observer. Each uncertainty is a 1σ random error, derived from the least-squares fit described in § III. Upper limits are 3σ .

K. We then ranked candidate sources according to the expected amplitude, z , of the Stokes V spectrum, which depends on line strength and width, as well as on B . We calculated the expected value for B assuming approximate equality of magnetic, kinetic, and gravitational energy densities, which gives,

$$B_{\text{eq}} = 15 \Delta v^2 / R \mu\text{G}, \quad (1)$$

where Δv is in km s^{-1} , and R is the cloud size in pc, as defined by the half-power contour (MGa). We identified the most promising sources to be B1 in Perseus, Taurus 16 in Taurus-Auriga, and NGC 2264 in Monoceros. We observed each with both polarization and frequency switching for 30–40 hr over a period of 3 weeks.

III. RESULTS

The results of all of our Zeeman observations are summarized in Table 1; and the B1 results are illustrated in Figure 1. As in previous Zeeman experiments (cf. Kazès and Crutcher 1986), field strength values were derived from a least-squares fit of a model to the observed Stokes V spectrum.⁷ The model is the sum of a scaling factor times the mean of the right and left circular line profiles (Stokes $I/2$) plus a scaling factor times the derivative of the line profile. The first scaling factor accounts

⁷ The Stokes V spectrum is a display of the right minus left circularly polarized signals. The sense of our left and right circular polarizations follows the IEEE definition; that is, right circular polarization is clockwise rotation of the electric vector as seen from the transmitter of the radiation.

for any gain difference which may exist between the right and left circularly polarized spectra. The second scaling factor is proportional to the magnitude of the Zeeman splitting, and hence, to the line-of-sight component of magnetic field strength, B_{\parallel} . The errors quoted in Table 1 correspond to the 1σ uncertainty in the fit.

In B1, a field of $-27 \pm 4 \mu\text{G}$ was detected. The derived field was independent of hour angle, which shows (for the rotating beam of an alt-az telescope) that the apparent Zeeman effect does not arise from a combination of source velocity gradient and separation of the right and left circular beam patterns along the direction of the gradient ("beam squint"). In Taurus 16 and NGC 2264, upper limits (3σ) of 18 and $15 \mu\text{G}$, respectively, were obtained. These small limits on B_{\parallel} imply a small value of B , a small component of B along the line of sight, or both. Taurus 16 and NGC 2264 will be discussed in more detail in a future paper.

Table 2 gives line width, map size, and column density in B1 for three different molecular transitions, ^{13}CO ($J = 1-0$), OH (1667 MHz), and NH_3 ($J, K = 1, 1$). In projection, the maps form concentric condensations of decreasing size, and emission from all three transitions peaks at about 6 km s^{-1} , indicating that the condensations are also coincident along the line of sight. The OH line width and size⁸ data were derived from the

⁸ Proximity of a second condensation to the north, and incomplete sampling to the southwest, prevent us from drawing a closed contour at the level of $0.50 \times (T_A)_{\text{max}}$. Instead, we show and measure R at outermost contours at the levels of 0.53 and $0.56 \times (T_A)_{\text{max}}$ for the 1665 and 1667 MHz lines, respectively.

TABLE 2
LINE WIDTH, CLOUD SIZE, COLUMN DENSITY, AND EQUILIBRIUM FIELD STRENGTHS IN BARNARD 1

LINE (1)	Δv (km s^{-1}) (2)	REFERENCE (3)	R (pc) (4)	REFERENCE (5)	N (10^{21} cm^{-2}) (6)	REFERENCE (7)	$B_{\text{eq}} (\mu\text{G})$		
							$4.2N$ (8)	$15 \Delta v^2 / R$ (9)	$7.4N^{3/4}$ (10)
$^{13}\text{CO}: J = 1 \rightarrow 0$	2.1	1	2.7	2	5	3	21	25	25
OH: 1667 MHz	1.3	4	1.1	4	6	3	25	23	28
$\text{NH}_3; J, K = 1, 1$	0.70	5	0.24	5	10	1	34	37	42

NOTE.— Δv is the FWHM of the spectral line profile; R is the geometric mean of the largest and smallest FWHM of the line intensity contour map; each is corrected for instrumental resolution. For ^{13}CO and OH, N is the mean visual extinction A_v , averaged over the half-power intensity contour, and converted to gas column density according to $N = 1 \times 10^{21} A_v \text{ cm}^{-2}$ (Bohlin, Savage, and Drake 1978). For NH_3 , N is the mean NH_3 column density, averaged over the half-power intensity contour, converted to gas column density according to $N = 1 \times 10^7 N(\text{NH}_3)$ (Benson and Myers 1983). For ^{13}CO and OH, expressions in cols. (8) and (9) for B_{eq} assume negligible thermal motions, as observed, and are based on eqs. (1) and (2) of MGa, respectively. For NH_3 , the kinetic temperature of 12 K (Bachiller *et al.* 1989) and line width of 0.70 km s^{-1} imply that thermal motions are not negligible: therefore each value of B_{eq} is multiplied by a correction factor of 1.2 for the value in col. (8), according to MGb, eq. (11), and 0.81 for the value in col. (9), according to MGb, eq. (8). The expression in col. (10) is based on the constant-mass evolutionary model of Mouschovias (1976, 1987a), assuming initial field strength $3 \mu\text{G}$ and a spherical cloud. (For a face-on disk of aspect ratio 2:1, B_{eq} in col. [10] would decrease by a factor of 1.1.)

REFERENCES.—(1) Bachiller and Cernicharo 1984; (2) Bachiller and Cernicharo 1986; (3) Cernicharo and Bachiller 1984; (4) this Letter; (5) Bachiller *et al.* 1989.

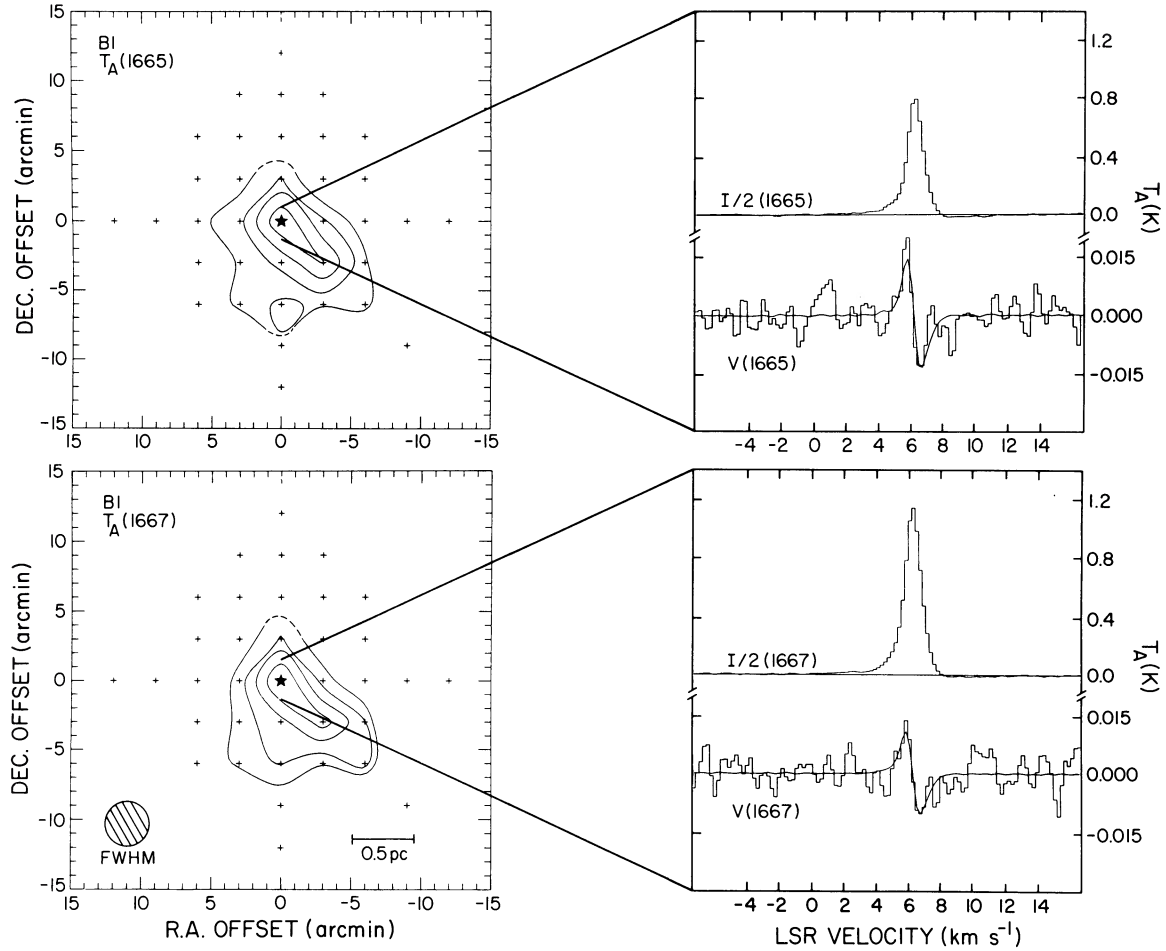


Fig. 1.—Summary of OH observations of B1. Panels at left show maps of 1665 and 1667 MHz OH emission in B1. Contours of T_A : 1665 map, 0.40, 0.50, 0.60, 0.70 K; 1667 map, 0.70, 0.85, 1.00, 1.15 K. Crosses indicate positions observed; additional emission (not shown) is present in the direction of the dashed contours. The filled star represents IRAS 03301 + 3057 (α [1950] = $3^{\text{h}}30^{\text{m}}10^{\text{s}}.5$; δ [1950] = $30^{\circ}57'47''$). Panels at right show the Stokes $I/2$ and Stokes V spectra for long-integration Zeeman observations of both transitions at the (0, 0) map position [α [1950] = $3^{\text{h}}30^{\text{m}}12^{\text{s}}.0$; δ [1950] = $30^{\circ}57'26''$]. Superposed on the V spectra are theoretical Zeeman patterns corresponding to a line-of-sight magnetic field strength of $-27 \mu\text{G}$ for 1665 MHz and $-25 \mu\text{G}$ for 1667 MHz.

spectra and maps shown in Figure 1. The corresponding column density is based on star counts, averaged over the OH half-power emission contour.⁹ The estimated uncertainties in Δv , R , and N , for the OH data, are 0.1 km s^{-1} , 0.3 pc , and $2 \times 10^{21} \text{ cm}^{-2}$. The column density listed in Table 2 under NH_3 is calculated from a derived column density of NH_3 , which is multiplied by an abundance ratio of 10^{-7} , a value generally appropriate for dark clouds like B1 (Benson and Myers 1983). The scatter in observed abundance ratios from one dark cloud to the next adds an uncertainty of at least a factor of 2 to the derived column density of the NH_3 condensation.

The line width, size, and column density information are used to estimate field strength in Table 2 in three distinct ways. In column (8), the assumption is made that the cloud is supported against gravity by magnetic energy, which causes B_{eq} to be directly proportional to N (Chandrasekhar and Fermi 1953;

⁹ The star count derived column density of $6 \times 10^{21} \text{ cm}^{-2}$, averaged over the OH half-power contour, agrees well with a value obtained from analysis of the 1665 and 1667 MHz OH lines as in Turner and Heiles (1971), using an abundance ratio of 3 OH molecules per 10^7 H_2 molecules, as in TMC 1 (Turner 1973). But since the OH abundance is obtained from comparison with star counts, we use the star count value directly.

MGa; MGb). The values listed in column (9) assume virial equilibrium *and* magnetic support (see MGa), which results in equation (1). The estimates in column (10) are based on the constant-mass evolutionary model of Mouschovias (1976a, b; 1987a), with an initial field strength $3 \mu\text{G}$ as suggested by Mouschovias (1987a). The numerical field strength predictions for each method are all remarkably similar.

The equilibrium field strengths in Table 2 apply to a progression of size scales: $\sim 3 \text{ pc}$ for ^{13}CO ; $\sim 1 \text{ pc}$ for OH; and $\sim 0.2 \text{ pc}$ for NH_3 . As the size scale decreases by a factor of ~ 10 , the gas density, $n \propto N/R$, increases by a factor of ~ 20 . Yet, B_{eq} increases by at most a factor of 1.6, from the 3 pc scale to the 0.2 pc scale, and this factor may not be significant given our measurement uncertainty. This weak dependence of B_{eq} on n may be consistent, at these size scales, with models of ambipolar diffusion (Shu, Adams, and Lizano 1987; Lizano and Shu 1988) and/or reconnection of field lines (Pringle 1988).

The calculations summarized in Table 2 indicate that the condensation traced by OH in B1 is in magnetic and virial equilibrium when a magnetic field $\sim 27 \mu\text{G}$ pervades the cloud. The similarity of all the estimated field strengths in Table 2, and their agreement within a factor ~ 2 , with the measured field strength, suggests that the gas in B1 may also be in

approximate magnetic and virial equilibrium over the range of size scales from 0.2 to 3 pc.

IV. DISCUSSION

B1 is part of a complex of dark clouds in Perseus, some 350 pc from the Sun (Herbig and Jones 1983). In visual extinction and in ^{13}CO emission, the complex has a projected extent of ~ 30 pc, and it consists of some 10 condensations, including B1, each with mean density $n \gtrsim 10^3 \text{ cm}^{-3}$, all connected by lower density molecular gas, with $n \sim 10^2 \text{ cm}^{-3}$ (Bachiller and Cernicharo 1984, 1986). The *IRAS* point source 03301 + 3057 lies near the peak of the NH_3 emission in B1 (Table 2; Bachiller and Cernicharo 1984), and its infrared spectrum rises toward long wavelengths, as is typical of an embedded protostar (Beichman et al. 1986). It is located at $\alpha(1950) = 3^{\text{h}}30^{\text{m}}10^{\text{s}}.5$; $\delta(1950) = 30^{\circ}57'47''$, approximately in the center of the beam of our Zeeman observations, and it has an *IRAS* luminosity of $3 L_{\odot}$. In its extinction, molecular line emission, and evidence for low-mass star formation, B1 resembles many of the condensations in nearby dark clouds.

In July of 1988, B1 was observed at the NRAO Green Bank 140 foot (42.7 m) telescope, using a procedure very similar to the one described in this *Letter*, and a field of $-19 \pm 3 \mu\text{G}$ was fitted to the Zeeman pattern found in the OH emission. This result is illustrated in Goodman et al. (1989) and will be discussed in more detail in a future paper.

It is now desirable to make OH Zeeman observations in other Perseus condensations similar to B1, to determine the field strength throughout the complex; to examine the extent to which virial and magnetic equilibrium apply; and to pursue the relation of magnetic fields and the process of low-mass star formation.

We are grateful to the staff of Arecibo Observatory for their support, to Michael Davis for his enthusiasm and many useful suggestions concerning our experiment, and to Karl Menten and Rafael Bachiller for providing NH_3 data in advance of publication. A. A. G. thanks Zonta International for an Amelia Earhart fellowship. Support to R. M. C. and T. H. T. is provided by NSF grant AST 86-11887.

REFERENCES

- Bachiller, R., and Cernicharo, J. 1984, *Astr. Ap.*, **140**, 414.
 ———. 1986, *Astr. Ap.*, **166**, 283.
 Bachiller, R., Martin-Pintado, J., Cernicharo, J., and Menten, K. 1989, in preparation.
 Beichman, C. A., Myers, P. C., Emerson, J. P., Harris, S., Mathieu, R. D., Benson, P. J., and Jennings, R. E. 1986, *Ap. J.*, **307**, 337.
 Benson, P. J., and Myers, P. C. 1983, *Ap. J.*, **270**, 589.
 Bohlin, R. C., Savage, B. D., and Drake, J. F. 1978, *Ap. J.*, **224**, 132.
 Cernicharo, J., and Bachiller, R. 1984, *Astr. Ap., Suppl.*, **58**, 327.
 Chandrasekhar, S., and Fermi, E. 1953, *Ap. J.*, **118**, 113.
 Crutcher, R. M. 1988, in *Molecular Clouds in the Milky Way and External Galaxies*, ed. R. L. Dickman, R. L. Snell, and J. Young (Berlin: Springer), in press.
 Crutcher, R. M., Kazès, I., and Troland, T. H. 1987, *Astr. Ap.*, **181**, 119.
 Crutcher, R. M., Troland, T. H., Kazès, I., Heiles, C., Goodman, A. A., and Myers, P. C. 1989, in preparation.
 Goodman, A. A., Myers, P. C., Crutcher, R. M., Heiles, C., Kazès, I., and Troland, T. H. 1989, in *The Physics and Chemistry of Interstellar Molecular Clouds*, ed. G. Winnewisser and J. T. Armstrong (Berlin: Springer), in press.
 Graedel, T. E., Langer, W. D., and Frerking, M. A. 1982, *Ap. J. Suppl.*, **48**, 321.
 Heiles, C. 1987, in *Interstellar Processes*, ed. D. Hollenbach and H. A. Thronson (Dordrecht: Reidel), p. 171.
 Herbig, G. H., and Jones, B. F. 1983, *A. J.*, **88**, 1040.
 Hildebrand, R. H. 1988, *Quart. J. R. A. S.*, in press.
 Kazès, I., and Crutcher, R. M. 1986, *Astr. Ap.*, **164**, 328.
 Lang, K. R., and Willson, R. F. 1979, *Ap. J.*, **227**, 163.
 Lizano, S., and Shu, F. H. 1988, *Ap. J.*, submitted.
 Mouschovias, T. Ch. 1976a, *Ap. J.*, **206**, 753.
 ———. 1976b, *Ap. J.*, **207**, 141.
 ———. 1987a, in *Physical Processes in Interstellar Clouds*, ed. G. Morfill and M. Scholer (Dordrecht: Reidel), p. 453.
 ———. 1987b, in *Physical Processes in Interstellar Clouds*, ed. G. Morfill and M. Scholer (Dordrecht: Reidel), p. 491.
 Myers, P. C., and Goodman, A. A. 1988a, *Ap. J. (Letters)*, **326**, L27.
 ———. 1988b, *Ap. J.*, **329**, 392.
 Pringle, J. E. 1988, *M. N. R. A. S.*, in press.
 Shu, F. H., Adams, F. C., and Lizano, S. 1987, *Ann. Rev. Astr. Ap.*, **25**, 23.
 Tamura, M. et al. 1987, in *Star Forming Regions*, ed. M. Peimbert and J. Jugaku (Dordrecht: Reidel), p. 48.
 Turner, B. E. 1973, *Ap. J.*, **186**, 357.
 Turner, B. E., and Heiles, C. 1971, *Ap. J.*, **170**, 453.
 Vrba, F. J., Strom, S. E., and Strom, K. M. 1976, *A. J.*, **81**, 958.

RICHARD M. CRUTCHER: Astronomy Department, University of Illinois, 341 Astronomy Building, 1011 West Springfield Avenue, Urbana, IL 61801

ALYSSA A. GOODMAN: Mail Stop 10, Harvard-Smithsonian Center for Astrophysics, 60 Garden Street, Cambridge, MA 02138

CARL HEILES: Astronomy Department, University of California, Berkeley, CA 94720

PHILIP C. MYERS: Mail Stop 42, Harvard-Smithsonian Center for Astrophysics, 60 Garden Street, Cambridge, MA 02138

THOMAS H. TROLAND: Physics-Astronomy Department, University of Kentucky, Lexington, KY 40506